

## Density profile of a quantized vortex line in superfluid ${}^4\text{He}^{\dagger\dagger}$

John H. Harper\* and Donald H. Kobe

*Department of Physics, North Texas State University, Denton, Texas 76203*

(Received 7 October 1974)

The relative-density amplitude profile of a quantized vortex line in He II is calculated from a generalized Gross-Pitaevskii (GP) equation. The ordinary GP equation is a Hartree nonlinear integrodifferential equation for the order parameter of an interacting system of bosons. The generalization is made by replacing the two-body potential in the average field by a local  $T$  matrix, which is calculated from a realistic interatomic potential for helium. In configuration space the  $T$  matrix is similar to the potential, except in the repulsive region where it is much softer. The only adjustable parameter in the generalized GP equation is the condensate fraction for which a theoretical value of 0.10 and an experimental value of 0.024 are used. In all cases the density profile is a monotonically increasing function with an effective core radius of from 3.7 to 4.7 Å.

### I. INTRODUCTION

One of the most remarkable developments in the microscopic theory of superfluidity was the prediction by Onsager<sup>1</sup> and Feynman<sup>2</sup> that vortices in He II should be quantized. The argument<sup>2</sup> is based on the single-valuedness of the condensate wave function,<sup>3</sup> and the quantum of circulation is shown to be  $h/m$ , where  $h$  is Planck's constant and  $m$  is the mass of the atom. Vinen<sup>4</sup> made the first attempt to observe quantized vortex lines using a vibrating wire. Although his results were indicative of vortex lines quantized in units of  $h/m$ , the later results of Whitmore and Zimmermann<sup>5</sup> confirmed that vortices are indeed quantized in integer multiples of  $h/m$ . By the nature of their apparatus, however, no information could be extracted about the structure of the vortex core.

In the meantime by a beautiful experiment on the motion of ions trapped in vortex rings, Rayfield and Reif<sup>6</sup> established conclusively that the circulation in He II is indeed quantized with a value of  $h/m$  to within experimental error. In order to obtain this value they used a classical model in which the vorticity is assumed to be constant within a core of radius  $a = 1.28 \pm 0.13$  Å. If a hollow core is assumed instead, they obtained a core radius of  $a = 1.00 \pm 0.10$  Å. The core radius is rather small compared to the interparticle separation. However the thermal de Broglie wavelength of the particles is large compared to the interparticle separation at a temperature of  $< 0.7$  K where the experiments were performed, so the fluid behaves in some respects like a continuum.

In order for the vortex ring to be a classical "quasiparticle" the group velocity must be the gradient of the energy with respect to the impulse

at constant volume or pressure. Roberts and Donnelly<sup>7</sup> used this concept to reanalyze the classical hydrodynamics of the vortex ring, and concluded that the radius of the hollow vortex core should be  $1.28 \pm 0.13$  Å in the vortex-ring experiment.<sup>6</sup> More recent experiments<sup>8</sup> in which the data are analyzed with the classical quasiparticle model have determined the vortex core radius more accurately to be  $1.28 \pm 0.05$  Å at 0.35 K. In addition, the pressure and temperature dependence of the vortex-core radius are also determined.<sup>8</sup> The value of the vortex-core radius extrapolated to 0 K is  $a = 1.14 \pm 0.05$  Å.<sup>8</sup> The temperature dependence agrees with a semi-phenomenological model based on a normal fluid core of a few angstroms, with a polarized tail of rotons outside the core.<sup>9</sup>

The vortex-core structure should be calculable from the quantum-mechanical theory of a many-boson system. In this paper it is calculated from a generalized Gross-Pitaevskii (GP) equation.<sup>10</sup> Other methods previously used are discussed later (Sec. VII) and compared with the results of the present calculation. The ordinary GP equation<sup>11,12</sup> is a nonlinear integrodifferential Hartree equation for the order parameter or condensate wave function. The potential between the particles in the condensate is taken into account by an average or mean field. In fact, for most realistic two-body potentials, the average field due to the other condensate particles is infinite. This divergence is due however to the absence of correlation between particles in the mean-field term of the GP equation, but this defect is partially remedied here.

Either a Hartree product wave function<sup>13</sup> or a canonical transformation<sup>12</sup> can be used to derive the GP equation. It was pointed out by Kobe<sup>10</sup>

that the average field in the GP equation is only the first term in a density amplitude and potential expansion of the actual average field in the equation of motion for the order parameter. By summing ladder diagrams in this expansion, a generalized GP equation is obtained in which the potential is replaced by the  $T$  matrix.<sup>14</sup> Even with potentials for which the Hartree field is infinite, the average field calculated from the  $T$  matrix is finite. In calculating the nonlocal  $T$  matrix, both Brueckner and Sawada<sup>14</sup> and Østgaard<sup>15</sup> use an energy denominator in which the particle kinetic energy is only partially dressed. However, in a recent calculation<sup>16</sup> of the excitation spectrum of He II, a local  $T$  matrix is derived in which the quasiparticle energy is used in the energy denominator.

In this paper the  $T$  matrix is calculated from the Morse dipole-dipole (MDD2) potential of Bruch and McGee.<sup>17</sup> The two different energy denominators used in the local  $T$  matrix calculation are (i) the particle kinetic energy minus the chemical potential, and (ii) the observed phonon-roton (quasiparticle) excitation spectrum.<sup>18</sup> Both  $T$  matrices approximate the potential for large interparticle separations, but are much softer in the repulsive core. When the condensate wave function (density amplitude) is calculated from the generalized GP equation, the only adjustable parameter is the fraction of the particles in the condensate. Of the two values for the condensate fraction used here, one value is the commonly quoted theoretical value of 0.10,<sup>19</sup> while the other is the recently measured experimental value of  $0.024 \pm 0.01$ .<sup>20</sup> The density amplitude is calculated with each of the two condensate fractions for each of the two  $T$  matrices. In each of these four cases the calculated density profile is monotonically increasing, with an effective core radius (the radius at which the density is half its asymptotic value) between 3.7 and 4.7 Å. These values are over three times the experimental radius of 1.14 Å,<sup>8</sup> which is discussed later. A preliminary account of this work has previously been given.<sup>21</sup>

In Sec. II, the generalized GP equation is derived by a factorization method. The  $T$  matrix, which plays the role of an effective interaction in

the generalized GP equation, is discussed in Sec. III. The generalized GP equation is written explicitly for a vortex line in Sec. IV. In Sec. V, which can be omitted in a first reading, the numerical methods used to solve the equations are briefly reviewed. The results are given in Sec. VI and discussed. In Sec. VII the results are compared with previous calculations. Finally, Sec. VIII gives the conclusions.

## II. GENERALIZED GROSS-PITAIEVSKII EQUATION

Since the ordinary GP equation<sup>11,12</sup> is a Hartree-like equation<sup>13</sup> for the condensate amplitude, no correlation is included. The effect of the interatomic interactions is taken into account only as an average or mean field due to all the other condensate particles, so the particles can come arbitrarily close to each other. Because of the strong interparticle repulsion at short distances, the particles should avoid each other. This lack of correlation between the particles manifests itself in an unphysical divergence of the mean field when a realistic potential is used. However, the interparticle correlations can be partially taken into account by replacing the bare potential by the  $T$  matrix. Just how this replacement can be mathematically justified is the subject of this section.

For a system of bosons, the order parameter or condensate wave function  $\phi(\vec{r}, t)$  at the position  $\vec{r}$  at the time  $t$  is postulated to be<sup>10</sup>

$$\phi(\vec{r}, t) = \langle \Psi_{N-1}(t) | \psi(\vec{r}) | \Psi_N(t) \rangle, \quad (2.1)$$

where  $\Psi_N(t)$  is the exact wave function for a system of  $N$  particles. The field annihilation and creation operators are  $\psi(\vec{r})$  and  $\psi^\dagger(\vec{r})$ , respectively, which satisfy the usual boson commutation relations.<sup>22</sup> The equation of motion for the order parameter can be obtained by using the  $N$ -body Schrödinger equation

$$H\Psi_N = i\hbar \frac{\partial \Psi_N}{\partial t}. \quad (2.2)$$

The Hamiltonian  $H$  in second quantization is given by<sup>22</sup>

$$H = \int d^3r \psi^\dagger(\vec{r}) (-\hbar^2/2m) \nabla^2 \psi(\vec{r}) + \int d^3r \psi^\dagger(\vec{r}) [U(\vec{r}) + U'(\vec{r}, t)] \psi(\vec{r}) \\ + \frac{1}{2} \int \int d^3r d^3r' \psi^\dagger(\vec{r}) \psi^\dagger(\vec{r}') V(\vec{r}, \vec{r}') \psi(\vec{r}') \psi(\vec{r}), \quad (2.3)$$

where  $U(\vec{r})$  is a static external field,  $U'(\vec{r}, t)$  is a time-dependent external field, and  $V(\vec{r}, \vec{r}') = V(|\vec{r} - \vec{r}'|)$  is the central two-body potential between the atoms. On differentiating Eq. (2.1) with respect to the time and using Eqs. (2.2) and (2.3), the equation of motion,

$$i\hbar \frac{\partial \phi(\vec{r}, t)}{\partial t} = -\left(\frac{\hbar^2}{2m}\right) \nabla^2 \phi(\vec{r}, t) + U(\vec{r})\phi(\vec{r}, t) + U'(\vec{r}, t)\phi(\vec{r}, t) + \int d^3r' V(\vec{r}, \vec{r}') \langle \Psi_{N-1}(t) | \psi^\dagger(\vec{r}') \psi(\vec{r}') \psi(\vec{r}) | \Psi_N(t) \rangle, \quad (2.4)$$

is obtained. The last term on the right-hand side of Eq. (2.4) gives the average time-dependent field due to all the other particles, which includes correlations between them. It has the graphical structure shown in Fig. 1.

If the correlation function in Eq. (2.4) is factorized into a product of three  $\phi$ 's, which would be valid for a weakly interacting boson system, the ordinary GP equation<sup>11,12</sup>

$$i\hbar \frac{\partial \phi(\vec{r}, t)}{\partial t} = -\left(\frac{\hbar^2}{2m}\right) \nabla^2 \phi(\vec{r}, t) + U(\vec{r})\phi(\vec{r}, t) + U'(\vec{r}, t)\phi(\vec{r}, t) + \int d^3r' V(\vec{r}, \vec{r}') \phi^*(\vec{r}', t) \phi(\vec{r}', t) \phi(\vec{r}, t) \quad (2.5)$$

is obtained. It is this equation that has been studied by a number of authors<sup>23,24</sup> with a  $\delta$ -function potential  $V(\vec{r}, \vec{r}') = V_0 \delta(\vec{r} - \vec{r}')$ , where  $V_0$  is an adjustable parameter. However, we will now take some of the correlation present in the exact wave functions in Eq. (2.4) into account.

In a previous paper,<sup>10</sup> it was shown that the exact wave functions of the system in Eq. (2.4) could be expanded in perturbation theory, and a selected class of diagrams summed to all orders to give a generalized GP equation

$$i\hbar \frac{\partial \phi(\vec{r}, t)}{\partial t} = \left(\frac{-\hbar^2}{2m}\right) \nabla^2 \phi(\vec{r}, t) + U(\vec{r})\phi(\vec{r}, t) + U'(\vec{r}, t)\phi(\vec{r}, t) + \int_{-\infty}^{\infty} dt' \int \int \int d^3r_2 d^3r_3 d^3r_4 \phi^*(\vec{r}_2, t) T(\vec{r}, \vec{r}_2, \vec{r}_3, \vec{r}_4, t-t') \phi(\vec{r}_3, t') \phi(\vec{r}_4, t'), \quad (2.6)$$

where  $T$  is in general a nonlocal  $T$  matrix.<sup>10</sup> This equation is a time-dependent Hartree equation with the potential  $V$  in Eq. (2.5) replaced by the  $T$  matrix.<sup>25</sup>

Equation (2.6) can be made more plausible by factorizing the exact expression in Fig. 1 into the approximation of Fig. 2. In Fig. 2 the small boxes represent the order parameter  $\phi$ . The approximation involved in Fig. 2 is that two particles are excited out of the single-particle condensate, interact in all ways permitted by the Hamiltonian (which, of course, includes noninteraction), finally interact once, and then one of the particles is reabsorbed into the condensate. If only free

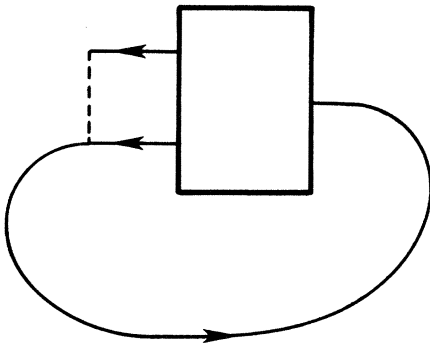


FIG. 1. Average field due to all the other particles given by the last term on the right-hand side of Eq. (2.4). The dashed line represents the two-body potential  $V$ , and the box represents the correlation function.

propagation and scatterings are allowed in the large box on the left-hand side, the  $T$  matrix is obtained on the right-hand side.

The  $T$  matrix satisfies an equation shown graphically in Fig. 3, and is expressed mathematically as<sup>10</sup>

$$T(1234) = V(1234) - \int d1' d2' d3' d4' V(121'2') \times iG_0(1', 3')G_0(2', 4')T(3', 4', 3, 4), \quad (2.7)$$

where  $(1) = (\vec{r}_1, t_1)$ ,  $(2) = (\vec{r}_2, t_2)$ , etc. The general two-body potential  $V$  is local in space and instantaneous in time, so

$$V(1234) = V(1, 2)\left(\frac{1}{2}\right) [\delta(1-3)\delta(2-4) + \delta(1-4)\delta(2-3)], \quad (2.8)$$

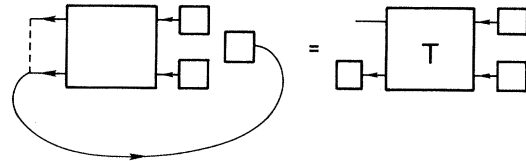


FIG. 2. Factorization of the correlation function in Fig. 1 to give the last term on the right-hand side of Eq. (2.6). The small boxes represent the order parameter  $\phi$ . If only free propagation and scatterings are allowed in the large box on the left-hand side, the  $T$  matrix is obtained on the right-hand side.

where the  $\delta$  function for both space and time is

$$\delta(1-3) = \delta(\vec{r}_1 - \vec{r}_3) \delta(t_1 - t_3), \quad (2.9)$$

and the local two-body potential is

$$V(1, 2) = V(\vec{r}_1, \vec{r}_2) \delta(t_1 - t_2). \quad (2.10)$$

The single-particle propagator  $G_0$  in Eq. (2.7) is given by<sup>10</sup>

$$G_0(1, 3) = \sum_n u_n(\vec{r}_1) u_n^*(\vec{r}_3) e^{-i\epsilon_n(t_1 - t_3)} \Theta(t_1 - t_3), \quad (2.11)$$

where  $\Theta$  is the step function which is unity for positive argument and zero otherwise. The single-particle functions  $\{u_n\}$  in Eq. (2.11) are eigenfunctions of a single-particle Hamiltonian,

$$[-\hbar^2/2m \nabla^2 + U(\vec{r})] u_n(\vec{r}) = \epsilon_n u_n(\vec{r}), \quad (2.12)$$

with eigenvalue  $\epsilon_n$ .

If the matrix elements of Eq. (2.7) are taken with respect to the single-particle functions  $\{u_n\}$ , followed by the time Fourier transform, the result is the usual equation<sup>25</sup> for the matrix elements of the  $T$  matrix,

$$\begin{aligned} \langle n_1 n_2 | T(\omega) | n_3 n_4 \rangle &= \langle n_1 n_2 | V | n_3 n_4 \rangle \\ &+ \sum_{n, m} \frac{\langle n_1 n_2 | V | nm \rangle \langle mn | T(\omega) | n_3 n_4 \rangle}{\omega - (\epsilon_n + \epsilon_m) + i0}, \end{aligned} \quad (2.13)$$

where  $\omega$  is the frequency. The  $T$  matrix is in general nonlocal and energy dependent. Equation (2.13) is extremely difficult to solve exactly, but in Sec. III a local approximation is made.

### III. EFFECTIVE INTERACTION

In this section the equation for a static local two-body  $T$  matrix is obtained from the general  $T$  matrix in Eq. (2.13). The approximations required are discussed, and a tractable equation for a  $T(|\vec{r}_1 - \vec{r}_2|)$  is obtained. This local  $T$  matrix simplifies tremendously the generalized GP equation in Eq. (2.6), and makes its solution feasible.

For the static local central two-body potential  $V(\vec{r}_1, \vec{r}_2) = V(|\vec{r}_1 - \vec{r}_2|)$  the matrix elements between plane-wave states are

$$\begin{aligned} \langle \vec{k}_1 \vec{k}_2 | V | \vec{k}_3 \vec{k}_4 \rangle &= (2\Omega)^{-1} [V(\vec{k}_1 - \vec{k}_4) + V(\vec{k}_1 - \vec{k}_3)] \\ &\times \delta_{\text{Kr}}(\vec{k}_1 + \vec{k}_2 - \vec{k}_3 - \vec{k}_4), \end{aligned} \quad (3.1)$$

where  $\Omega$  is the volume of the system and momentum conservation is insured by the Kronecker delta  $\delta_{\text{Kr}}$ , which is unity for zero argument and



FIG. 3. Graphical representation of the  $T$ -matrix integral equation in Eq. (2.7).

zero otherwise. The Fourier transform of the potential is defined as

$$V(\vec{k}) = V(|\vec{k}|) = \int d^3r e^{-i\vec{k} \cdot \vec{r}} V(|\vec{r}|). \quad (3.2)$$

The external potentials  $U$  and  $U'$  in Eq. (2.3) are taken to be zero, and periodic boundary conditions are imposed, so that the solutions of Eq. (2.12) are a complete set of plane-wave states.

A static ( $\omega = 0$ ) local  $T$  matrix can be obtained from Eq. (2.13) by using plane waves and setting  $\vec{k}_3 = \vec{k}_4 = 0$ , which gives

$$\begin{aligned} \langle \vec{k}, -\vec{k} | T | 00 \rangle &= \langle \vec{k}, -\vec{k} | V | 00 \rangle \\ &+ \sum_{\vec{p}} \frac{\langle \vec{k}, -\vec{k} | V | -\vec{p}, \vec{p} \rangle \langle \vec{p}, -\vec{p} | T | 00 \rangle}{-2\epsilon_p}, \end{aligned} \quad (3.3)$$

on using momentum conservation. Since the local  $T$  matrix can be written in the form of Eq. (3.1), Eq. (3.3) then becomes

$$T(k) = V(k) - \frac{1}{\Omega} \sum_{\vec{p}} \frac{V(\vec{k} + \vec{p}) T(p)}{2\epsilon_p}. \quad (3.4)$$

Equation (3.4) can also be obtained from the Bogoliubov canonical<sup>26</sup> transformation, except that the energy denominator is the quasiparticle energy  $E_p$ , not the bare energy  $\epsilon_p$ .<sup>16</sup> This similarity gives justification in dressing the energy denominator, which corresponds to using the dressed propagators in the intermediate states in Fig. 3.

Since the integral in Eq. (3.4) is of the convolution form, the inverse transform of Eq. (3.4) is the integral equation

$$T(r) = V(r) \left( 1 - \int_0^\infty dr' L(r, r') T(r') \right), \quad (3.5)$$

where the kernel is

$$L(r, r') = \frac{r'}{\pi r} \int_0^\infty dp \epsilon_p^{-1} \sin p r \sin p r'. \quad (3.6)$$

Equation (3.5) is more easily solved than Eq. (3.4), since the Fourier transform of  $V(r)$ , which has a strong repulsive core, need not be taken.

From Eq. (3.6) it can be seen that as  $r \rightarrow \infty$  the kernel in Eq. (3.5) vanishes, so that

$$T(r) \rightarrow V(r) \text{ as } r \rightarrow \infty. \quad (3.7)$$

Thus the  $T$  matrix is expected to depart signifi-

cantly from  $V(r)$  only at short distances where the strong repulsive core induces strong short-range correlations into the wave function.

The generalized GP equation in Eq. (2.6) can now be written with  $U=U'=0$  as

$$i\hbar \frac{\partial \phi(\vec{r}, t)}{\partial t} = \left( \frac{-\hbar^2}{2m} \right) \nabla^2 \phi(\vec{r}, t) + \int d^3r' T(|\vec{r} - \vec{r}'|) \times \phi^*(\vec{r}', t) \phi(\vec{r}', t) \phi(\vec{r}, t), \quad (3.8)$$

when the local static central  $T$  matrix approximation in Eq. (3.5) is used, along with Eqs. (2.8)–(2.10). In Sec. IV, Eq. (3.8) is written explicitly for a vortex line.

#### IV. VORTEX-LINE EQUATION

The generalized GP equation in Eq. (3.8) has solutions which describe a vortex line. To find these solutions the condensate wave function  $\phi(\vec{r}, t)$  is chosen to be of the form<sup>12,23</sup>

$$\phi(\vec{r}, t) = (n_0)^{1/2} f(\rho) e^{i l \theta} e^{-i \mu t}, \quad (4.1)$$

in cylindrical coordinates  $(\rho, \theta, z)$ , where  $\mu$  is the chemical potential,  $n_0$  is the condensate density, and  $l$  is the number of quanta of circulation. The function  $f(\rho)$  is the relative condensate density amplitude at a distance  $\rho$  from the vortex axis. If Eq. (4.1) is substituted into Eq. (3.8), the equation for the relative density amplitude  $f(\rho)$  is

$$\frac{d^2 f(\rho)}{d\rho^2} + \rho^{-1} \frac{df(\rho)}{d\rho} - l^2 \rho^{-2} f(\rho) + \bar{\mu} f(\rho) - \bar{n}_0 \int_0^\infty d\rho' \rho' K(\rho, \rho') f(\rho')^2 f(\rho) = 0, \quad (4.2)$$

where  $\bar{\mu} = 2m\mu/\hbar^2$  and  $\bar{n}_0 = 2mn_0/\hbar^2$ . Since vortex lines with one quantum of circulation have the lowest energy,  $l$  is taken to be unity here. The kernel in Eq. (4.2) is itself a double integral,

$$K(\rho, \rho') = 4 \int_0^\pi d\theta \int_0^\infty dz \times T((\rho^2 + \rho'^2 - 2\rho\rho' \cos\theta + z^2)^{1/2}), \quad (4.3)$$

because the vortex line has cylindrical symmetry while the  $T$  matrix has spherical symmetry.

The chemical potential  $\mu$  can be determined from the boundary condition at infinity. The relative density amplitude  $f(\rho)$  approaches the bulk density at large distances from the vortex core, so

$$f(\rho) \rightarrow 1, \quad f'(\rho) \rightarrow 0, \quad f''(\rho) \rightarrow 0 \quad \text{as } \rho \rightarrow \infty. \quad (4.4)$$

Therefore, from Eq. (4.2) the chemical potential is given by

$$\mu = n_0 \lim_{\rho \rightarrow \infty} \int_0^\infty d\rho' \rho' K(\rho, \rho') f(\rho')^2. \quad (4.5)$$

In contrast to the positive chemical potential obtained by using a repulsive  $\delta$ -function potential,<sup>13,23</sup> Eq. (4.5) can be negative, which would indicate a bound system. The second boundary condition is that  $f(0)=0$  at the origin, since otherwise an infinite energy would be obtained. In Sec. V the numerical methods used to solve for the  $T$  matrix and the relative condensate density amplitude are discussed. The reader who is primarily interested in the results of the calculation can skip to Sec. VI.

#### V. NUMERICAL METHODS

In this section the numerical methods used in solving the equations of Secs. III and IV are briefly discussed. It is beyond the scope of this paper to discuss the numerical procedures in full detail, which is done elsewhere.<sup>27</sup> The method of solving Eq. (3.5) for the  $T$  matrix is first briefly discussed, followed by the method for obtaining the kernel  $K(\rho, \rho')$  in Eq. (4.3). Finally the method of solving Eq. (4.2) for the density amplitude  $f(\rho)$  is outlined.

Since a realistic potential  $V(r)$  is strongly repulsive at short distances, Eq. (3.5) for  $T(r)$  is divided by  $V(r)$ , and then the resulting equation is solved for the ratio  $T(r)/V(r)$ . The potential  $V(r)$  used here is the Morse dipole-dipole-2 (MDD2) potential of Bruch and McGee.<sup>17</sup> The kernel  $L(r, r')$  in Eq. (3.6) is numerically evaluated for two different energy denominators  $\epsilon_p$ : (i) the bare particle energy  $p^2/2m$  minus the experimental<sup>28</sup> chemical potential  $-6.7$  K, and (ii) the experimental phonon-roton excitation spectrum  $E_p$ .<sup>18</sup> To simplify the calculation of  $L(r, r')$ , Eq. (3.6) can be written

$$\frac{\pi r}{r'} L(r, r') = \int_0^b dp \epsilon_p^{-1} \sin pr \sin pr' + \frac{1}{2} \int_b^\infty dp \epsilon_p^{-1} \cos p(r-r') - \frac{1}{2} \int_b^\infty dp \epsilon_p^{-1} \cos p(r+r') \quad (5.1)$$

For case (i) the limit  $b$  can be taken as zero, since at  $p=0$  the denominator is finite. However, for case (ii) the denominator is zero at  $p=0$ , so it is convenient to choose  $b=2 \text{ \AA}^{-1}$ , below which the phonon and roton regions occur. The integrals with the cosines in Eq. (5.1) are evaluated using the IBM eight-point Gaussian quadrature<sup>29</sup> for

each quarter-period of the cosine function. The integration is terminated when the contribution of one complete period is less than  $10^{-5}$  of the accumulated sum of terms. The integral from 0 to  $b$  is also performed by using the IBM eight-point Gaussian quadrature<sup>29</sup> for every  $0.2\text{-}\text{\AA}^{-1}$  increment. Evenly spaced values of  $r$  and  $r'$  between 0 and  $10\text{ \AA}$  are used. The number of different values of  $r$  and  $r'$  depends on the number needed for the solution of Eq. (3.5).

The method of solution of Eq. (3.5) for  $T(r)$  is similar to the Fredholm procedure for integral equations of the second kind.<sup>30</sup> The integral equation is converted into a set of  $n$  linear algebraic equations for equispaced  $r_i$  ( $i=1, 2, \dots, n$ ) in the interval between 0 and  $10\text{ \AA}$ . This set of equations is solved simultaneously by using a maximum pivot strategy in Gauss-Jordan complete elimination.<sup>31</sup> Numerical solutions of systems of linear equations for large  $n$  may not be accurate due to increased round-off and truncation errors. Therefore, Eq. (3.5) for the first energy denominator was solved for  $n=20, 34, 50$ , and  $100$ . For  $n=100$  the change in the values of  $T(r_i)$  over  $n=50$  was less than 1 part in  $10^3$ , so convergence is assured for  $n=100$ . For the second energy denominator Eq. (3.5) was solved for  $T(r)$  with  $n=100$ . As a final check the calculated values of  $T(r_i)$  were substituted into the set of equations obtained from Eq. (3.5) to ensure that it was indeed satisfied.

The next step is to calculate the kernel  $K(\rho, \rho')$  in Eq. (4.3) from the  $T$  matrix. Since the  $T$  matrix is spherically symmetric and the vortex line is cylindrically symmetric, the kernel  $K(\rho, \rho')$  is a double integral—one over the  $z$  direction along the axis of the vortex line and the other over the azimuthal angle. An adaptive Newton-Cotes integration method<sup>32</sup> is used for both integrals in Eq. (4.3). For each value of the azimuthal angle used in the integration, the infinite  $z$  integration is performed by comparing the value between the limits  $2^{n-1}$  and  $2^n\text{ \AA}$  ( $n=1, 2, 3, \dots$ ) with the accumulated total from 0 to  $2^{n-1}\text{ \AA}$ . When the ratio is less than 1 part in  $10^4$  the procedure terminates. The adaptive Newton-Cotes method breaks the  $z$  integration from  $2^{n-1}$  to  $2^n$  into a sufficient number of subintervals so that convergence to 1 part in  $10^3$  is obtained. The same procedure is used for the azimuthal integration from 0 to  $\pi$ . The symmetric matrix  $K(\rho_i, \rho'_j)$  is calculated for  $\rho_i, \rho'_j$  between 0 and  $13\text{ \AA}$  with a step size of  $0.2\text{ \AA}$ .

The generalized GP equation in Eq. (4.2) can be written in discrete form between 0 and  $9\text{ \AA}$  in steps of  $0.2\text{ \AA}$  using finite differences for the derivatives and the repeated use of a Newton-Cotes six-point

closed formula<sup>33</sup> for the integral. The two boundary conditions are  $f(0)=0$  and  $f(9\text{ \AA})=c \leq 1$ . The value of  $c$  is chosen to be 0.98, but the density profile is not sensitive to variations in it between  $+0.015$  and  $-0.03$ .

The integral in Eq. (4.2), which extends to infinity, is evaluated in three regions. For  $\rho'$  between 0 and  $9\text{ \AA}$ , the kernel  $K(\rho_i, \rho'_j)$  is multiplied by  $f(\rho'_j)^2$ . For  $\rho'$  between 9 and  $13\text{ \AA}$ ,  $f(\rho')$  is taken to be Fetter's approximation<sup>34</sup>  $\rho'(\rho'^2 + a^2)^{-1/2}$  for  $a=1.3\text{ \AA}$ . Beyond  $\rho'=13\text{ \AA}$ ,  $f(\rho'_j)$  is taken to be unity. The kernel  $K$  in Eq. (4.3) is calculated in this region by approximating  $T$ , which is essentially  $V$ , by a series expansion in  $\rho/\rho'$ . The upper limit is chosen sufficiently large ( $\sim 30\text{ \AA} < \rho' < \sim 50\text{ \AA}$ ) so that further extension caused no appreciable change in the integral.

The set of algebraic equations obtained by writing Eq. (4.2) in discrete form is solved by the method of perturbed parameters.<sup>35</sup> First the set of equations is solved for a condensate density  $n_0=0$ . The differential equation in Eq. (4.2) for  $l=1$  with  $n_0=0$  has a solution which is a Bessel function of order 1 for  $\mu > 0$ , and a modified Bessel function of order 1 for  $\mu < 0$ . The solution is substituted to evaluate the integral term in Eq. (4.2), and the equation set is solved again for a nonzero value of  $n_0$ .<sup>36</sup> Usually four or five iterations are required for self-consistency. This process is repeated until the value of  $n_0$  is increased to its final value of either  $0.024n$  or  $0.10n$ , where the density<sup>37</sup> of the bulk He II extrapolated to zero temperature and pressure is  $n=0.0218$  atoms  $\text{\AA}^{-3}$ . Usually four or five different evenly spaced values of  $n_0$  between zero and the final value are required to obtain the solution.

The set of algebraic equations obtained from Eq. (4.2) is solved for various values of the chemical potential  $\mu$ . The value of  $\mu$  for which  $f'(9\text{ \AA})$  is approximately zero ( $0+$ ) is chosen, so that the boundary condition in Eq. (4.4) is satisfied. The results of these calculations are given in Sec. VI.

## VI. RESULTS AND DISCUSSION

In this section the results of the calculations for the  $T$  matrix and the density amplitude are given and discussed. The  $T$  matrix is calculated with two different energy denominators in Eq. (3.6). Then for each of these two  $T$  matrices, the density amplitude  $f$  is calculated from the generalized GP equation in Eq. (4.2) with two different condensate densities. The two different  $T$  matrices obtained are now discussed.

The  $T$  matrix shown in Fig. 4 is obtained when the energy denominator  $\epsilon_p = p^2/2m + 6.7\text{ K}$ , where

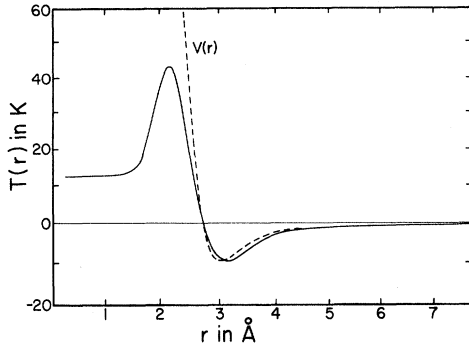


FIG. 4. Local  $T$  matrix in configuration space, calculated by using the energy denominator  $\epsilon_p = p^2/2m + 6.7$  K. The dashed curve is the MDD2 potential in Ref. 17.

$-6.7$  K is the experimental chemical potential,<sup>28</sup> is used for the kernel in Eq. (3.6). The strong repulsive part of the MDD2 potential<sup>17</sup>  $V(r)$  shown by the dashed curve in Fig. 4 induces strong short-range correlations in the wave function, which causes it to vanish if the particles are sufficiently close. The  $T$  matrix is an effective interaction for use with the unperturbed wave function, which takes this short-range correlation in the true wave function into account. Therefore, for short distances  $T(r)$  is much softer than the bare potential, as shown in Fig. 4. For distances beyond about  $2.5$  Å the  $T(r)$  approaches  $V(r)$ , as expected from Eq. (3.7). The  $T(r)$  shown in Fig. 4 is very similar to the  $T$  matrix plotted by Østgaard,<sup>38</sup> although his  $T$  matrix is not local.

When the experimental phonon-roton spectrum<sup>18</sup> is used in Eq. (3.6) for the kernel in Eq. (3.5) for the  $T$  matrix, the  $T$  matrix shown in Fig. 5 is obtained. The  $T$  matrix is about the same as Fig. 4 beyond about  $2.5$  Å, but is larger for values of

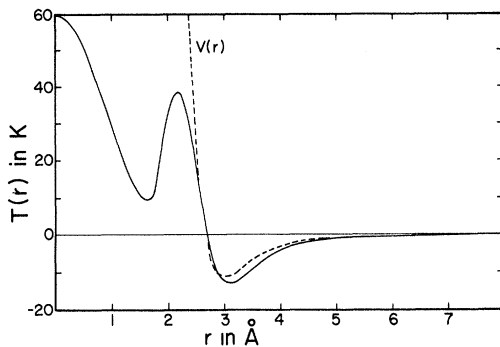


FIG. 5. Local  $T$  matrix in configuration space, calculated by using the observed phonon-roton spectrum in Ref. 18 as the energy denominator. The dashed curve is the MDD2 potential in Ref. 17.

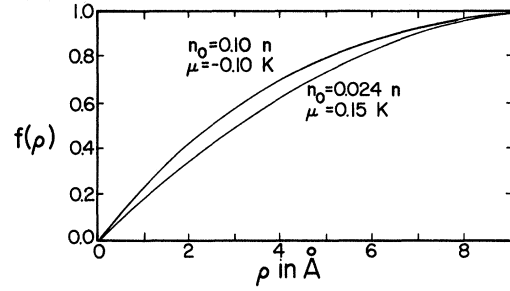


FIG. 6. Relative density amplitude  $f(\rho)$  for a vortex line as a function of the distance  $\rho$  from the axis calculated from the  $T$  matrix in Fig. 4 for two different condensate densities  $n_0$ . The bulk density of He II is  $n = 0.0218$  Å<sup>-3</sup> at 0 K and 0 atm.

$r$  less than about  $1$  Å.

The density amplitude  $f(\rho)$  for the vortex line is calculated from the generalized GP equation in Eq. (4.2). The kernel in Eq. (4.3) is calculated from the  $T$  matrix given in Fig. 4. Then the density amplitudes  $f$  shown in Fig. 6 are obtained. Two different values of the condensate density have been used. A value of the condensate fraction  $n_0/n = 0.1$  has been calculated by several groups.<sup>19</sup> On the other hand, recent experiments<sup>20</sup> have indicated that a value of  $n_0/n = 0.024 \pm 0.01$  is the physical value. Both of these values are used in the calculations given here. The value of the bulk density  $n$  used is  $0.0218$  atoms Å<sup>-3</sup>, corresponding to the density of He II extrapolated to zero temperature and pressure.<sup>37</sup>

For a condensate density  $n_0 = 0.10 n$  the density amplitude profile shown in the upper curve of Fig. 6 is obtained, which is a monotonically increasing function. The effective core radius is defined to be the distance  $a$  from the vortex line for which the density  $n(a)$  is half the bulk density  $0.5 n$ , which corresponds to a relative density amplitude of  $f(a) = 0.707$ . The effective vortex core radius is then  $4.2$  Å, which is over three times larger than the experimental value<sup>8</sup> of  $1.14$  Å extrapolated to 0 K. The chemical potential for which the boundary condition in Eq. (4.4) is satisfied is  $\mu = -0.10$  K. The negative value of the average energy per particle  $\mu$ , although small, indicates that the system is bound.

For the experimental value<sup>20</sup> of the condensate density  $n_0 = 0.024 n$ , another solution was found for the relative density amplitude  $f(\rho)$  in Eq. (4.2) with the  $T$  matrix of Fig. 4, which is shown in the bottom curve of Fig. 6. The effective core radius obtained is  $4.7$  Å, somewhat larger than the previous case. However, the chemical potential obtained is  $0.15$  K, which, although small,

indicates that the system is not bound.

The  $T$  matrix in Fig. 5, obtained by using the observed phonon-roton spectrum as the denominator in Eq. (3.6), is also used to calculate the density amplitude  $f(\rho)$ . The kernel in Eq. (4.3) is calculated from the  $T$  matrix, which in turn is used in the generalized GP equation in Eq. (4.2) for the density amplitude  $f(\rho)$  of a vortex line. The same two condensate densities  $n_0$  used in Fig. 6 are used here also.

When Eq. (4.2) is solved for  $n_0 = 0.10 n$ , the density amplitude shown in the upper curve in Fig. 7 is obtained. It is a monotonically increasing function with an effective vortex core radius of  $3.7 \text{ \AA}$ , which is somewhat less than the corresponding value obtained in Fig. 6. The chemical potential satisfying the boundary condition in Eq. (4.4) is  $\mu = -0.48 \text{ K}$ , which indicates that the system is bound.

When the condensate density  $n_0 = 0.024 n$  is used, the density amplitude shown in the lower curve of Fig. 7 is obtained. It is also a monotonically increasing function, having an effective vortex core radius of  $4.4 \text{ \AA}$ . The chemical potential obtained is  $\mu = 0.08 \text{ K}$ , which indicates a slightly unbound system.

In all cases in Figs. 6 and 7 the effective vortex core radii are over three times greater than the experimental value<sup>8</sup> of  $1.14 \text{ \AA}$ . These results are discussed further in Sec. VIII. However, in Sec. VII a comparison is made between this work and other approaches to the density profile of a quantized vortex line.

#### VII. COMPARISON WITH OTHER WORK

The calculations of Sec. VI are compared here with other calculations of the density profile of a quantized vortex line. Previously, two different methods have been used to obtain the density profile.

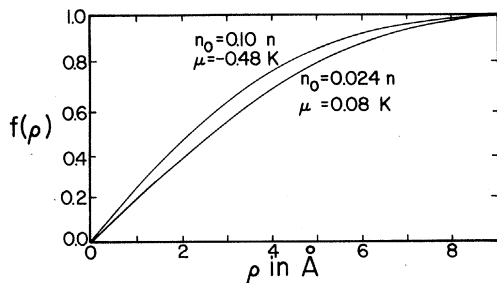


FIG. 7. Relative density amplitude  $f(\rho)$  for a vortex line as a function of the distance  $\rho$  from the axis calculated from the  $T$  matrix in Fig. 5 for two different condensate densities  $n_0$ . The bulk density of He II is  $n = 0.0218 \text{ \AA}^{-3}$  at  $0 \text{ K}$  and  $0 \text{ atm}$ .

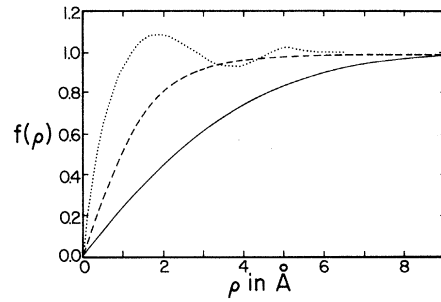


FIG. 8. Relative density amplitude calculated in this work from Fig. 7 with  $n_0 = 0.1 n$  (solid curve), calculated from the Gross-Pitaevskii equation with a  $\delta$ -function potential in Ref. 40 (dashed curve), and calculated from a correlated wave function in Ref. 41 (dotted curve).

The first method which was used is the ordinary GP equation in Eq. (2.5) with a  $\delta$ -function potential of strength  $V_0$ .<sup>23</sup> Although other authors<sup>39</sup> have used an equation like this one to calculate the density profile, the most accurate calculations have been made by Kawatra and Pathria.<sup>40</sup> The  $V_0$  is absorbed into a "healing length" and adjusted to give a vortex core radius of about  $1.6 \text{ \AA}$ . Their monotonically increasing density profile is shown by the dashed curve in Fig. 8. The chemical potential in this approach is always positive, which indicates an unbound system, and is deduced to be about  $\mu = 6 \text{ K}$ .

A second approach to the density profile of a quantized vortex line has been used by Chester, Metz, and Reatto.<sup>41</sup> They use a model wave function which, in addition to including short-range correlations, vanishes on the core of the vortex line and has one quantum of circulation around the axis. When this model wave function is used in connection with the energy variational principle, and the experimental liquid structure factor is inserted into their approximate equations, they obtain the relative density amplitude shown by the dotted curve in Fig. 8. The effective core radius is about  $0.5 \text{ \AA}$ , but for another trial function a core radius of about  $0.8 \text{ \AA}$  is obtained. Oscillations in the density, reminiscent of the pair correlation function, are obtained,<sup>41</sup> which Chester<sup>42</sup> explains in terms of particle correlations. The density, of course, is not expected to have the same behavior as the pair correlation function. Even though the average interparticle spacing is about  $3.5 \text{ \AA}$  and the distance of closest approach of two atoms is about  $2.7 \text{ \AA}$ , it is not surprising that the vortex core can be about  $1 \text{ \AA}$ . At temperatures  $< 0.7 \text{ K}$  the thermal de Broglie wavelength of the particles is much larger than the average interparticle spacing, so the condensate can be considered essentially as a continuum.



Thus the density is essentially a constant in the absence of the vortex line. However, when a vortex line is present the energy is minimized if a core of radius  $\sim 1 \text{ \AA}$  exists in the condensate. A simpler variational calculation of Amit and Gross<sup>43</sup> based on a Hartree energy functional using the  $\delta$ -function potential gives the value of  $1.7 \text{ \AA}$  for the core radius.

### VIII. CONCLUSION

The density profile for a quantized vortex line is obtained here using a  $T$  matrix<sup>25</sup> calculated from a realistic potential as the effective interaction in the Gross-Pitaevskii (GP) equation.<sup>10</sup> Thus some correlation induced by the two-body potential is taken into account in what would otherwise be a Hartree independent-particle model.<sup>13</sup> The calculation of the density profile has been made for two different  $T$  matrices calculated from the Morse dipole-dipole (MDD2) potential.<sup>17</sup> For the energy denominator, the kinetic energy minus the chemical potential is used in one case, whereas the observed phonon-roton spectrum<sup>18</sup> is used for the other case. In the calculation of the density amplitude, the only adjustable parameter is the condensate fraction  $n_0/n$ , for which two values are used. One value is the commonly quoted theoretical value<sup>19</sup> of 0.10, while the other value is the recently determined experimental value<sup>20</sup> of 0.024. The relative density amplitude in all four cases considered is a monotonically increasing function with an effective core radius (radius at half-maximum density) of between  $3.7$  and  $4.7 \text{ \AA}$ . The calculated chemical potentials are slightly negative for a condensate fraction of 0.10, and slightly positive for a condensate fraction of 0.024. The negative chemical potential indicates a bound system, which the previous calculations<sup>40</sup> based on the GP equation do not give. It is perhaps disappointing that the theory here gives a vortex core which is over three times the experimental value<sup>8</sup> extrapolated to 0 K, which is  $1.14 \text{ \AA}$ . On the other hand, it is remarkable that even an order-of-magnitude agreement is obtained, since a calculation with the bare MDD2 potential<sup>17</sup> in the GP equation did not converge. Thus it is necessary to take the multiple scattering of two particles into account to obtain a convergent density profile.

There are several conceptual difficulties connected with the method used here. One difficulty is that the method deals only with the particles in the condensate. For a weakly interacting inhomogeneous boson system Fetter<sup>44</sup> has shown that the core should be partially filled with pairs of noncondensate particles with total angular momentum zero. Even though the condensate density

is zero in the core, he shows that the density of the noncondensate particles in the core is approximately 1.4 times the density of the noncondensate particles in the bulk.<sup>45</sup> Fetter<sup>46</sup> then conjectures that for HeII the same qualitative behavior could occur. Since the condensate fraction in HeII is only 0.024, as measured recently,<sup>20</sup> the fraction of particles not in the condensate is 0.976. Thus if the conjecture is correct, the total density in the vortex core would be greater than the bulk HeII. Fetter<sup>45</sup> then suggests a more sophisticated trial wave function than that used by Chester, Metz, and Reatto<sup>41</sup> to take this effect into account for HeII. However, this effect could also be taken into account by using the pair and single-particle condensate theory<sup>47</sup> with a realistic potential or a  $T$  matrix calculated from it.

An objection to the use of the ordinary GP equation is that it is a mean field equation, which does not take into account interparticle correlations. This criticism<sup>41</sup> is obviated by the generalized GP equation<sup>10</sup> used here which does take interparticle correlations into account through the use of the  $T$  matrix.<sup>25</sup> Since at very low temperatures the thermal de Broglie wavelength of the particles in the condensate is very long compared to the interparticle spacing, the condensate behaves very much like a continuum. Therefore, it is expected that the generalized GP equation would provide a good description of the vortex structure, even down to the range of  $1 \text{ \AA}$  or less. However, it is in principle possible to calculate higher-order corrections to the generalized GP equation used here.<sup>10</sup> The monotonic increase in the density amplitude is not unexpected. The oscillations in the density profile obtained by Chester, Metz, and Reatto<sup>41</sup> are unexplained in their original paper, but ascribed to particle correlations by Chester.<sup>42</sup>

Although the temperature and pressure dependence of the vortex core radius have been measured experimentally,<sup>8</sup> it is not immediately obvious how to calculate these dependencies from the generalized GP equation.<sup>10</sup> The condensate density  $n_0$  is a function of the temperature and pressure, but its dependence has not yet been measured. In light of the small value<sup>20</sup> of the condensate density there are even those who doubt that the zero-momentum state is in fact macroscopically occupied, contrary to most theoretical approaches. A temperature-dependent local  $T$  matrix could be calculated both by using the temperature-dependent phonon-roton spectrum in the energy denominator and multiplying the integrand in Eq. (3.6) by a factor of  $\coth(\epsilon_p/2k_B T)$ , where  $k_B$  is the Boltzmann constant and  $T$  is the absolute temperature. On the basis of previous

calculations of the temperature dependence of the excitation spectrum,<sup>16</sup> this approach does not seem to be especially fruitful. Perhaps a unification of the GP equation with the Ginzburg-Pitaevskii equation<sup>39</sup> can be made which would be valid at temperatures intermediate between the transition temperature and zero. Since the vortex core calculated here at zero temperature is over three times larger than the experimental value, it does not seem to be fruitful at this time to pursue the above refinements.

In order to decide between the various density profiles shown in Fig. 8, resort must be made to experiment. Even though vortex lines have been directly observed recently,<sup>48</sup> no information on the core structure is obtained from the experiment. An irregular array of lines is seen,<sup>48</sup> instead of a triangular lattice<sup>49</sup> of vortex lines. Perhaps the irregular array of vortices can be pinned in a regular lattice, and the form factor for an individual vortex line extracted from neutron or x-ray scattering data. Vortex lines in He II are by no means as well understood as the analogous flux lines in type-II superconductors.<sup>50</sup> Obviously there are many problems remaining to obtain a thorough understanding of vortices in He II, which will provide a challenge for both theorists and experimentalists for many years to come.

*Note added in proof.* The effective core radius determined here is not directly comparable with the core radius determined experimentally. The classical hydrodynamic analysis of Rayfield and Reif<sup>6</sup> involves the fluid density for which they use  $0.1454 \text{ g cm}^{-3}$  or  $n = 0.02187 \text{ atoms } \text{Å}^{-3}$ . In our calculation the condensate density  $n_0$  enters, for which the values of  $0.1n$  and  $0.024n$  were used. When a calculation with the condensate density equal to the bulk density was attempted, the solution did not converge. The good agreement between the classical analysis of Rayfield and Reif<sup>6</sup> and experiment indicates that the particles not in the condensate are coupled to it and also participate in the vortex motion. In our calculation the particles not in the condensate have been neglected. Hall<sup>51</sup> has inferred that the core radius of a free vortex line is  $(6.8 \pm 1.6) \text{ Å}$  from experiments on the velocity of vortex waves. Rayfield and Reif<sup>6</sup> suggest that the presence of a charge on the core of their vortex rings may modify the effective core radius compared to that of an uncharged vortex line.

#### ACKNOWLEDGMENTS

We would like to thank Dr. G. W. Goble for many discussions during the course of this work. For a careful reading of the manuscript, we are grateful to W. P. Latham, Jr.

†Work supported in part by the North Texas State University Faculty Research Fund.

‡Based in part on a dissertation submitted by one of us (J.H.H.) to North Texas State University in partial fulfillment of the requirements for the Ph.D. degree.

\*Present address: Science Division, Angelina College, Lufkin, Tex. 75901.

<sup>1</sup>L. Onsager, *Nuovo Cimento Suppl.* **6**, 279 (1949). In a footnote to a paper on statistical hydrodynamics Onsager writes on p. 281, "Vortices in a suprafluid [*sic*] are presumably quantized; the quantum of circulation is  $h/m$ , where  $m$  is the mass of a single molecule."

<sup>2</sup>R. P. Feynman, in *Progress in Low Temperature Physics*, edited by C. J. Gorter (North-Holland, Amsterdam, 1955), Vol. 1, Chap. II.

<sup>3</sup>E. Merzbacher, *Am. J. Phys.* **30**, 237 (1962).

<sup>4</sup>W. F. Vinen, *Proc. R. Soc. A* **260**, 218 (1961).

<sup>5</sup>S. C. Whitmore and W. Zimmermann, Jr., *Phys. Rev.* **166**, 181 (1968); *Phys. Rev. Lett.* **15**, 389 (1965).

<sup>6</sup>G. W. Rayfield and F. Reif, *Phys. Rev.* **136**, A1194 (1964); *Phys. Rev. Lett.* **11**, 305 (1963).

<sup>7</sup>P. H. Roberts and R. J. Donnelly, *Phys. Lett. A* **31**, 137 (1970).

<sup>8</sup>W. I. Glaberson and M. Steingart, *Phys. Rev. Lett.* **26**, 1423 (1971); M. Steingart and W. I. Glaberson, *J. Low Temp. Phys.* **8**, 61 (1972); *Phys. Rev. A* **5**, 985 (1972).

<sup>9</sup>W. I. Glaberson, D. M. Strayer, and R. J. Donnelly, *Phys. Rev. Lett.* **21**, 1740 (1968).

<sup>10</sup>D. H. Kobe, *Phys. Rev. A* **5**, 854 (1972). See this paper for background and previous references to the Gross-Pitaevskii equation.

<sup>11</sup>E. P. Gross, *Ann. Phys. (N.Y.)* **9**, 292 (1960).

<sup>12</sup>L. P. Pitaevskii, *Zh. Eksp. Teor. Fiz.* **40**, 646 (1961) [*Sov. Phys.—JETP* **13**, 45 (1961)].

<sup>13</sup>E. P. Gross, *J. Math. Phys.* **4**, 195 (1963).

<sup>14</sup>K. A. Brueckner and S. Sawada, *Phys. Rev.* **106**, 1117 (1957); **106**, 1128 (1957).

<sup>15</sup>E. Østgaard, *J. Low Temp.* **4**, 239 (1971).

<sup>16</sup>G. W. Goble and D. H. Kobe, *Phys. Rev. A* **10**, 851 (1974).

<sup>17</sup>L. W. Bruch and I. J. McGee, *J. Chem. Phys.* **52**, 5884 (1970). They give two Morse dipole-dipole potentials with different parameters, which are called MDD1 and MDD2. The MDD2 potential is recommended for condensed-state calculations.

<sup>18</sup>R. A. Cowley and A. D. B. Woods, *Can. J. Phys.* **49**, 177 (1971).

<sup>19</sup>W. P. Francis, G. V. Chester, and L. Reatto, *Phys. Rev. A* **1**, 86 (1970); O. Penrose and L. Onsager, *Phys. Rev.* **104**, 576 (1956); W. L. McMillan, *ibid.* **138**, A442 (1965); D. Schiff and L. Verlet, *ibid.* **160**, 208 (1967).

<sup>20</sup>H. A. Mook, R. Scherm, and M. K. Wilkinson, *Phys. Rev. A* **6**, 2268 (1972); H. A. Mook, *Phys. Rev. Lett.* **32**, 1167 (1974). The latter reference obtains a value of  $(1.8 \pm 1)\%$  which is compatible with the value  $(2.4 \pm 1)\%$  obtained in the former.

- <sup>21</sup>J. H. Harper and D. H. Kobe, *Bull. Am. Phys. Soc.* **19**, 674 (1974); D. H. Kobe and J. H. Harper, *ibid.* **17**, 518 (1972).
- <sup>22</sup>For a discussion of second quantization see, e.g., D. H. Kobe, *Am. J. Phys.* **34**, 1150 (1966).
- <sup>23</sup>E. P. Gross, *Nuovo Cimento* **20**, 454 (1961).
- <sup>24</sup>For examples and an extended list of references, see e.g., E. P. Gross, in *Physics of Many-Particle Systems*, Vol. 1, edited by E. Meeron (Gordon and Breach, New York, 1966), pp. 263-338.
- <sup>25</sup>See, e.g., N. H. March, W. H. Young, and S. Sampathar, *The Many-Body Problem in Quantum Mechanics* (Cambridge University Press, Cambridge, 1967), pp. 192-201.
- <sup>26</sup>D. H. Kobe, *Ann. Phys. (N.Y.)* **47**, 15 (1968).
- <sup>27</sup>J. H. Harper, Ph.D. dissertation (North Texas State University, Denton, 1975) (unpublished).
- <sup>28</sup>K. R. Atkins, *Liquid Helium* (Cambridge U. P., Cambridge, England, 1959), pp. 21-23.
- <sup>29</sup>IBM Corporation, *System/360 Scientific Subroutine Package* (Technical Publications Dept., 112 E. Post Rd., White Plains, N. Y., 1968), p. 301.
- <sup>30</sup>L. P. Smith, *Mathematical Methods for Scientists and Engineers* (Prentice-Hall, Englewood Cliffs, N.J., 1953), pp. 380-387.
- <sup>31</sup>B. Carnahan, H. A. Luther, and J. O. Wilkes, *Applied Numerical Methods* (Wiley, New York, 1969), pp. 272-296.
- <sup>32</sup>P. J. Davis and P. Rabinowitz, *Numerical Integration* (Blaisdell, Waltham, Mass., 1967), pp. 164-165, 198.
- <sup>33</sup>See Ref. 31, p. 74. This method is the extension of Simpson's rule to six points.
- <sup>34</sup>A. L. Fetter, *Phys. Rev.* **138**, A429 (1965).
- <sup>35</sup>F. Freudenstein and B. Roth, *Assoc. Comp. Mach. J.* **18**, 550 (1963).
- <sup>36</sup>The equation set is solved by iteration until the difference between successive approximate solutions is less than  $10^{-5}$ .
- <sup>37</sup>J. Wilks, *The Properties of Liquid and Solid Helium* (Clarendon, Oxford, 1967).
- <sup>38</sup>E. Østgaard, *J. Low Temp. Phys.* **4**, 585 (1971), Figs. 1 and 2.
- <sup>39</sup>A similar calculation was made previously for an equation with the same form as the GP equation, but valid only near the transition temperature. See V. L. Ginzburg and L. P. Pitaevskii, *Zh. Eksp. Teor. Fiz.* **34**, 1240 (1958) [*Sov. Phys.-JETP* **7**, 858 (1958)].
- <sup>40</sup>M. P. Kawatra and R. K. Pathria, *Phys. Rev.* **151**, 132 (1966).
- <sup>41</sup>G. V. Chester, R. Metz, and L. Reatto, *Phys. Rev.* **175**, 275 (1968).
- <sup>42</sup>G. V. Chester, in *Lectures in Theoretical Physics*, edited by K. T. Mahanthappa and W. E. Brittin (Gordon and Breach, New York, 1969), Vol. XIB, pp. 271-279.
- <sup>43</sup>D. Amit and E. P. Gross, *Phys. Rev.* **145**, 130 (1966). They state that a  $\delta$ -function potential is used because "the potential-energy integral is hopelessly complicated even for the simplest  $V(\vec{x} - \vec{y})$ ."
- <sup>44</sup>A. L. Fetter, *Phys. Rev. Lett.* **27**, 986 (1971).
- <sup>45</sup>A. L. Fetter, *Ann. Phys. (N.Y.)* **70**, 67 (1972).
- <sup>46</sup>A. L. Fetter, in Ref. 42, pp. 365-366.
- <sup>47</sup>D. H. Kobe, *J. Math. Phys.* **10**, 1507 (1969).
- <sup>48</sup>G. A. Williams and R. E. Packard, *Phys. Rev. Lett.* **33**, 280 (1974).
- <sup>49</sup>D. Stauffer and A. L. Fetter, *Phys. Rev.* **168**, 156 (1967). Although they show that a triangular lattice has a lower energy than a rectangular lattice, they conclude that in the real situation the lattice would unlikely be regular.
- <sup>50</sup>See, e.g., L. Leplae, H. Umezawa, and F. Mancini, *Phys. Lett. C* **10**, 151 (1974).
- <sup>51</sup>H. E. Hall, *Adv. Phys.* **9**, 89 (1960).